Coexistence of Dominant Marine Phytoplankton Sustained by Nutrient Specialization

Takako Masuda,[a,b]* Keisuke Inomura,[c] Jan Mareš,[b,d,e] Taketoshi Kodama,[a] Takuhei Shiozaki,[a]§ Takato Matsui,[f] Koji Suzuki,[f] Shigenobu Takeda,[a]◇ Curtis Deutsch,[g] Ondřej Prášil,[b] Ken Furuya[a]∞

[a]Department of Aquatic Bioscience, The University of Tokyo, Bunkyo, Tokyo, Japan

[b]Institute of Microbiology, The Czech Academy of Sciences, Třeboň, Czechia

[c]Graduate School of Oceanography, University of Rhode Island, Narragansett, Rhode Island, USA

[d]Institute of Hydrobiology, Biology Centre of the Czech Academy of Sciences, České Budejovice, Czechia

[e]Department of Botany, University of South Bohemia, Faculty of Science, České Budejovice, Czechia

[f]Graduate School of Environmental Science/Faculty of Environmental Earth Science, Hokkaido University, Sapporo, Japan

[g]Department of Geosciences, Princeton University, Princeton, New Jersey, USA

Takako Masuda and Keisuke Inomura contributed equally to the article. The order of the two authors was determined based on the chronology of the study.

ABSTRACT *Prochlorococcus* and *Synechococcus* are the two dominant picocyanobacteria in the low-nutrient surface waters of the subtropical ocean, but the basis for their coexistence has not been quantitatively demonstrated. Here, we combine *in situ* microcosm experiments and an ecological model to show that this coexistence can be sustained by specialization in the uptake of distinct nitrogen (N) substrates at low-level concentrations that prevail in subtropical environments. In field incubations, the response of both *Prochlorococcus* and *Synechococcus* to nanomolar N amendments demonstrates N limitation of growth in both populations. However, *Prochlorococcus* showed a higher affinity to ammonium, whereas *Synechococcus* was more adapted to nitrate uptake. A simple ecological model demonstrates that the differential nutrient preference inferred from field experiments with these genera may sustain their coexistence. It also predicts that as the supply of NO_3^- decreases, as expected under climate warming, the dominant genera should undergo a nonlinear shift from *Synechococcus* to *Prochlorococcus,* a pattern that is supported by subtropical field observations. Our study suggests that the evolution of differential nutrient affinities is an important mechanism for sustaining the coexistence of genera and that climate change is likely to shift the relative abundance of the dominant plankton genera in the largest biomes in the ocean.

IMPORTANCE Our manuscript addresses the following fundamental question in microbial ecology: how do different plankton using the same essential nutrients coexist? *Prochlorococcus* and *Synechococcus* are the two dominant picocyanobacteria in the low-nutrient surface waters of the subtropical ocean, which support a significant amount of marine primary production. The geographical distributions of these two organisms are largely overlapping, but the basis for their coexistence in these biomes remains unclear. In this study, we combined *in situ* microcosm experiments and an ecosystem model to show that the coexistence of these two organisms can arise from specialization in the uptake of distinct nitrogen substrates; *Prochlorococcus* prefers ammonium, whereas *Synechococcus* prefers nitrate when these nutrients exist at low concentrations. Our framework can be used for simulating and predicting the coexistence in the future ocean and may provide hints toward understanding other similar types of coexistence.

KEYWORDS nutrient specialization, *Prochlorococcus*, *Synechococcus*

Marine phytoplankton are key drivers of the global carbon cycle (1, 2), photosynthesizing about 50×10^{15} g carbon (C) annually, which is comparable to that of the global terrestrial biosphere (1). Nearly a quarter of this net primary production can be accounted for by the two marine cyanobacteria *Prochlorococcus* and *Synechococcus* (3). The geographical distributions of the two groups are largely overlapping in the latitude band from $\sim$40°N to $\sim$40°S (4). Because of their dominance in such vast oceanic regions, understanding their niche partitioning is critical in predicting the future ecosystem and biogeochemical cycling. However, how these organisms coexist has still been in question.

Nutrient utilization is a critical factor in microbial coexistence (5–7). In the stratified open ocean, nutrient supply is weak, and concentrations are commonly drawn down to nanomolar levels that limit the rates of growth and uptake by phytoplankton (8). In these biomes, the mechanisms by which phytoplankton species partition scarce resources determine the relative abundance of species and thus community composition. However, a long-standing theory predicts that the species whose nutrient acquisition saturates at the lowest concentration will drive other organisms to extinction (9), such that coexistence requires specialization on distinct nutrient resources. Qualitative evidence supports differential nitrogen utilization in *Prochlorococcus* and *Synechococcus* (10), but the traits and conditions that favor the coexistence or dominance of these genera have not yet been quantitatively demonstrated. For example, models that assume similar nitrogen affinities for *Prochlorococcus* and *Synechococcus* (11) promote competitive exclusion, even where coexistence is widely observed (e.g., in the North Atlantic Gyre) (3).

To quantify the causes of niche separation and coexistence of *Prochlorococcus* and *Synechococcus*, we conducted a suite of nutrient enrichments at a nanomolar level to simulate realistic perturbations at a fixed station in the North Pacific (12°N, 135°E). The North Pacific subtropical gyre, where *Prochlorococcus* and *Synechococcus* are numerically predominant in the phytoplankton community, is characterized by extremely low surface nutrient concentrations at the nanomolar level with temporal and spatial variation (6, 12–15). We analyzed the data on growth and nutrient uptake using a simple population model for each species and applied the model to determine whether the coexistence of these species can be maintained.

RESULTS AND DISCUSSION

***In situ* experiments.** To test the effect of increased nutrients at the nanomolar level, we conducted five nitrogen (N) addition experiments (M1 to M5) at the surface of a station in the subtropical Northwestern Pacific (12°N, 135°E) from 6 to 25 June 2008 during the MR08-02 cruise aboard the R/V *MIRAI*. Grazing was eliminated by filtration (see details in Materials and Methods) so that changes in phytoplankton abundance could be considered cell growth or cell death. To verify that only N was limiting, we also conducted three Fe-addition (Fe1 to Fe3) experiments (Table S8 in reference 16). Neither P nor Fe enrichment increased the abundance of any of the tested phytoplankton groups, including *Prochlorococcus* and *Synechococcus* (Fig. 1; see Fig. S1A and B and Table S1 in the supplemental material). Initial nutrient concentrations remained low during the cruise ($<$45 nM for N, $\sim$30 nM for P, and more than 0.1 nM for dissolved iron) (see Table S2 in the supplemental material).

With the N addition, the growth of both *Prochlorococcus* and *Synechococcus* was stimulated regardless of its chemical form (repeated measures analysis of variance [RM-ANOVA], $\alpha < 0.05$) (Fig. 1; Fig. S1C and D; Table S1; see Table S3 in the supplemental material). However, the magnitude of growth responses differed between the oxidized and reduced forms of N, and these differences were genus specific (Fig. 1; Fig. S1C and D; Table S1 and S3). The growth of *Prochlorococcus* was more stimulated by ammonium (NH_4^+), while *Synechococcus* responded more strongly to nitrate (NO_3^-) (Fig. 1; Table S3). The enriched NH_4^+ was depleted on the third day, leading to decreased populations in both organisms (Fig. 1; see Fig. S2 in the supplemental
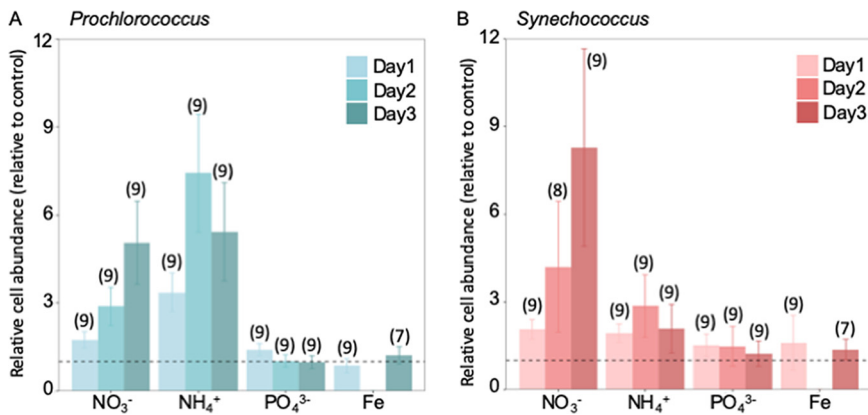
FIG 1 The effects of different chemical forms of N, P, and Fe additions on cell abundances of *Prochlorococcus* (A) and *Synechococcus* (B) relative to controls (means $\pm$ SD), with the number of samples in parentheses. For N and P addition, data are based on experiments M1 to M3, where the initial concentrations of N were small (<10 nM) (Table S2). It shows that *Prochlorococcus* prefers NH_4^+ while *Synechococcus* prefers NO_3^-. Note that added NH_4^+ was depleted on the third day, leading to decreased populations in both organisms (Fig. S2). The dotted line at 1 represents no change from the control.

material). Urea stimulated the growth of *Prochlorococcus* and *Synechococcus* similar to or sometimes better than ammonium or nitrate, respectively (Fig. S1C and D; Table S3).

Prochlorococcus showed a significantly higher peak abundance in the NH_4^+ additions relative to the NO_3^- additions in all five N and P bioassays (RM-ANOVA, $P < 0.05$) (Fig. 1; Fig. S1C; Table S3), indicating a higher affinity to NH_4^+ than to NO_3^-. This affinity difference can be explained by the low electron requirement to assimilate NH_4^+, which has been shown previously in *Prochlorococcus* both in culture and *in situ* (17–19).

Unlike *Prochlorococcus*, *Synechococcus* increased in the NO_3^- amendment significantly more than in any other N treatments at the nanomolar level (ANOVA, $\alpha < 0.05$) (Fig. 1B: Fig. S1D; Table S3). The preference for NO_3^- over NH_4^+ among *Synechococcus* has been consistent with results of the previous *in situ* bioassay experiments in the oligotrophic North Pacific Subtropical Gyre (17). A preference for NO_3^- over NH_4^+ among *Synechococcus* seems at odds with both the energetic advantage of reduced N and with the direct observations in pure culture, which showed faster growth on NH_4^+ when NH_4^+ is relatively abundant (19, 20). The following modeling exercise reconciles these apparently conflicting observations, based on the differentiated half-saturation constants and affinity for NO_3^- and NH_4^+.

Ecological model for N uptake preferences. To discern the mechanisms that sustain the coexistence of *Prochlorococcus* and *Synechococcus*, we used a simple ecological model (6, 7, 21, 22). The model represents distinct physiological traits for growth and nutrient affinity for each population and allows for their ecological interaction for the following two different N resources: NH_4^+ and NO_3^-. We have selected NO_3^- and NH_4^+ to be part of the model mainly to focus on delivering the most striking finding extracted from the data—the different affinity to chemical forms of inorganic nitrogen between two organisms. Inorganic nutrients are also more commonly used in ecological modeling, and we have followed the previous similar studies focusing on inorganic nutrients (6, 7).

Despite its simplicity, the model reproduces the observed trends in populations over the course of the field study (Fig. 2; Fig. S3). The key parameters of the model were half-saturation constants (K) (see Table S4 in the supplemental material). K values have been thought to represent the density of transporters on the cellular surface (23–25), with a lower value representing a higher transporter density. A lower K_{NH4} for *Prochlorococcus* was essential to reproduce the rapid *Prochlorococcus* growth up to day 2 and the slower *Synechococcus* growth with NH_4^+ addition (Fig. 2A); when the species' relative NH_4^+ affinities are reversed, the model results deviate from the data (see Fig. S4 in the supplemental material). On the other hand, K for NO_3^- (K_{NO3}) must be lower
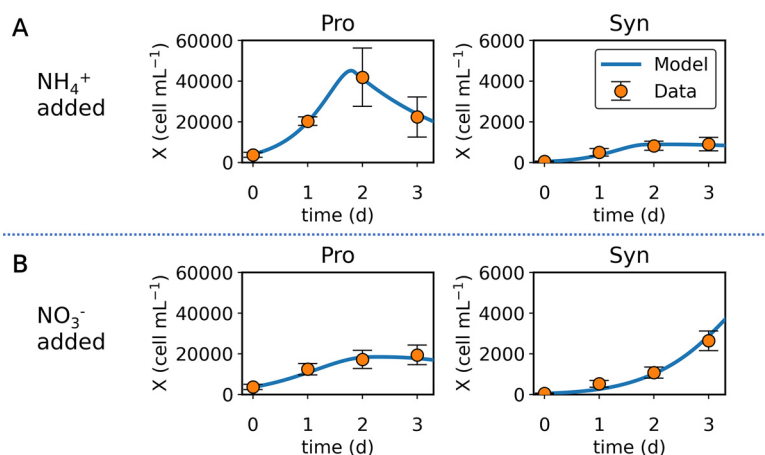
FIG 2 Model data comparison of the time series of the abundance (X) of *Prochlorococcus* and *Synechococcus*. (A) NH_4^+ added. (B) NO_3^- added. Points, data; curves, model; Pro, *Prochlorococcus*; Syn, *Synechococcus*. Data are based on experiments M1 to M3, where the initial concentrations of N were small (<10 nM) (Table S2). The error bars represent the standard deviation based on the mean values across from the selected experiments.

for *Synechococcus* to reproduce its continued high growth up to day 3 (Fig. 2B), and a reversal of species NO_3^- affinities again results in a poor model fit to the data (see Fig. S5 in the supplemental material). Decreased K_{NO3} of *Prochlorococcus* also causes model results to diverge from the data (compare Fig. 2 and Fig. S5).

The model parametrization suggests a higher maximum uptake (V_{max}) of NO_3^- by *Synechococcus* than that of *Prochlorococcus* (Table S4), which also may contribute to the niche differentiation. It also indicates that V_{max} for NH_4^+ is higher than that for NO_3^- both for *Prochlorococcus* and *Synechococcus*. Thus, under high nutrient concentrations, *Synechococcus* may grow faster with NH_4^+ than with NO_3^- (Table 1; Fig. 3). This model implication is consistent with the previous experiments where a large amount (micromolar level) of NH_4^+ and NO_3^- is added (19, 20). However, the affinity ($A = V_{max}/K$) for NO_3^- turned out to be higher than that for NH_4^+ for *Synechococcus* (see Table S5 in the supplemental material). The affinity provides an alternative measure of the relative ability of various species to compete for nutrients (24, 26). Because the affinity is the initial slope of nutrient uptake versus nutrient concentration relationship (27), the value of affinity is especially relevant when nutrients are depleted as in the subtropical gyres, where small phytoplankton tend to dominate (28). The result shows *Synechococcus* has an advantage for NO_3^- and *Prochlorococcus* has an advantage for NH_4^+ (Table S5), consistent with what is suggested by the predicted half-saturation values (and not by maximum uptake rates). These results collectively suggest that in a low-nutrient environment as in the subtropical gyres, these organisms have different nitrogen uptake preferences for NH_4^+ and NO_3^- (Table 1; Fig. 3), allowing their coexistence, and the differentiated half-saturation constants are the key contributors.

To test the effect of different affinity and K values on the coexistence of *Prochlorococcus* and *Synechococcus*, we obtained a steady-state solution for cellular nitrogen per volume of water for various ratios of $K_{NO3}^{Pro}/K_{NO3}^{Syn}$ and $K_{NH4}^{Pro}/K_{NH4}^{Syn}$ (note that these relationships are the inversely

TABLE 1 Preferred nutrient for *Prochlorococcus* and *Synechococcus* under different nutrient concentrations

Genus	Preferred nutrient under:	
	Low-nutrient concentration[a]	High-nutrient concentration[a]
Prochlorococcus	NH_4^+	NH_4^+
Synechococcus	NO_3^-	NH_4^+

[a]Broadly, low nutrient indicates lower nanomolar level (e.g., surface of subtropical gyres [e.g., this study]) and high nutrient indicates above that level (e.g., initial conditions of batch culture experiments [19, 20, 96]). Specifically, the nutrient preference of *Synechococcus* is predicted to be flipped at 39 nM (Fig. 3).
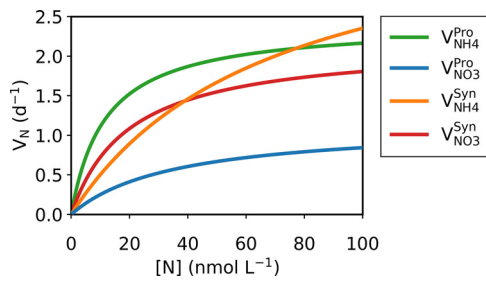
FIG 3 Nutrient uptake rate V_N against nutrient concentration $[N]$. In the legend, *Pro* and *Syn* indicate *Prochlorococcus* and *Synechococcus*, respectively, and *NH4* and *NO3* indicate ammonium and nitrate, resepectively. For example, V_{NH4}^{Pro} indicates ammonium uptake rate by *Prochlorococcus* versus ammonium concentrations.

proportional to the affinity ratios given the constant V_{max} values). The result shows that these K value ratios strongly influence the coexistence of these organisms at given resource ratios of NO_3^- and NH_4^+. For example, when the resource ratio of NO_3^- and NH_4^+ is 1:3, the model shows that the set of K values that reproduce the observations (Fig. 1, 2) allows coexistence with a similar amount of biomass, where *Prochlorococcus* uses mainly NH_4^+ and *Synechococcus* uses mainly NO_3^- (see the cyan triangle in Fig. 4A and the domain explanation in Fig. 4B, zone i). If $K_{NO3}^{Pro}/K_{NO3}^{Syn}$ was lower, we would expect to see only *Prochlorococcus* (Fig. 4B, zone iii); however, if $K_{NH4}^{Pro}/K_{NH4}^{Syn}$ was sufficiently higher, *Synechococcus* would exclude *Prochlorococcus* by outcompeting them for NH_4^+ (Fig. 4B, zone ii). If both $K_{NO3}^{Pro}/K_{NO3}^{Syn}$ was lower and $K_{NH4}^{Pro}/K_{NH4}^{Syn}$ was higher, an alternative state of coexistence could persist (Fig. 4B, zone i). However, this scenario would require *Synechococcus* to prefer NH_4^+ at low concentrations, which would be in violation of our incubation results.

Preferential grazing by zooplankton (e.g., nanoflagellates [29]) or virus (30, 31) may further ensure the coexistence of these species (32–35). However, our study shows that, without reliance on zooplankton behavior, *Prochlorococcus* and *Synechococcus* have inherent nutrient-based mechanisms for coexistence.

The lower K value for NO_3^- in *Synechococcus* than that for *Prochlorococcus* predicts that their relative abundance will also depend strongly on the NO_3^-/NH_4^+ ratio of the nutrient supply (Fig. 5A). We tested this model prediction using field observations from the Hawaii Ocean Timeseries (HOT [36]) in the subtropical North Pacific (Fig. 5B). We find that the ratio cell counts of *Prochlorococcus* to *Synechococcus* exhibit a strong relationship to ambient NO_3^- concentration (Fig. 5B). This finding is consistent with a previously observed positive relationship between nanomolar NO_3^- concentrations at the surface and *Synechococcus* abundance but not for *Prochlorococcus* abundance (37–39). A *Synechococcus* bloom was also observed after the transient nanomolar increase of surface NO_3^- in the stratified
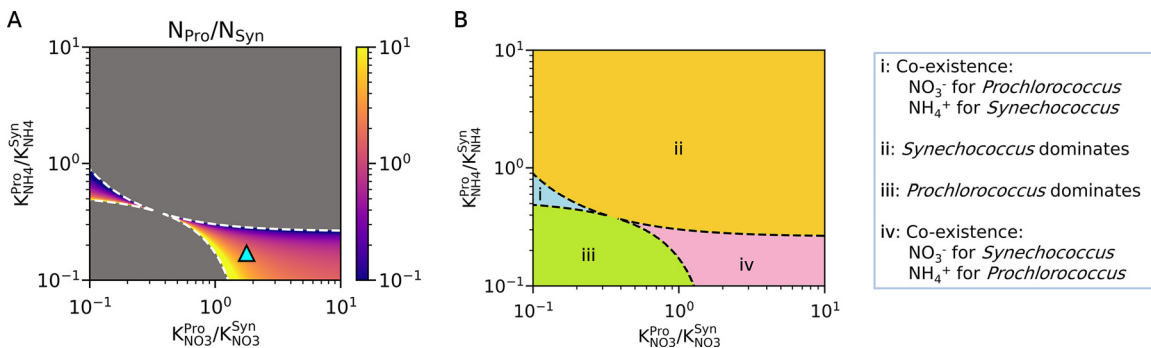
FIG 4 Steady-state solution of the model for the coexistence of *Prochlorococcus* and *Synechococcus* based on the ratios of half-saturation constants for nitrogen sources. (A) Model results of the ratio of *Prochlorococcus* and *Synechococcus* expressed in terms of the proportion of total cellular nitrogen concentration in the water (N_{Pro}/N_{Syn}, see the color bar for values). The cyan triangle in A represents the optimized ratios of the half-saturation constants predicted from Fig. 2. The model output is based on the resource ratio of NO_3^- and NH_4^+ that is 1:3 (for other ratios, see Fig. 5 and Fig. S6), which allows the coexistence of these organisms with the optimized ratios. Dashed curves indicate borders between coexistence and noncoexistence. (B) Explanation of each domain; coexistence occurs only in domains i and iv.
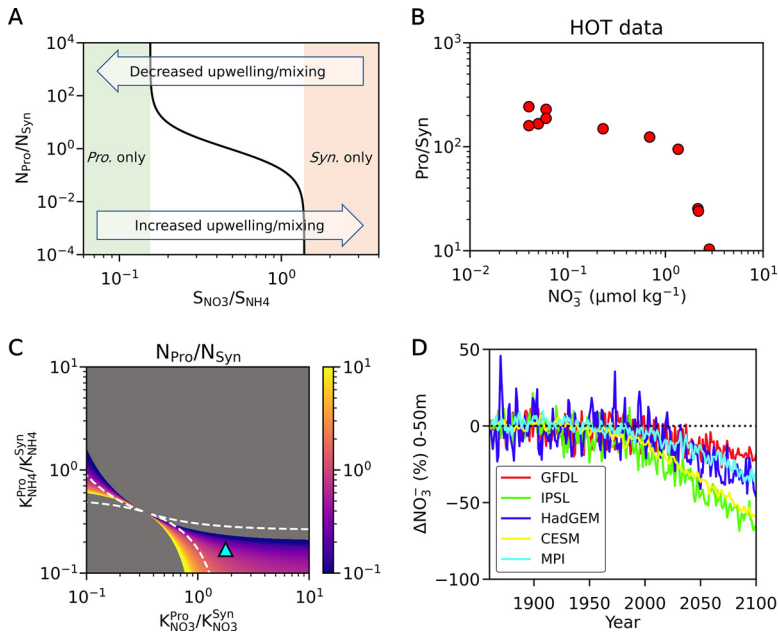
FIG 5 Resource-ratio-based shifts of coexistence. (A) The shift in the ratio of *Prochlorococcus* and *Synechococcus* based on the resource ratios of $NO_3^-:NH_4^+$ (S_{NO3}/S_{NH4}) with the predicted half-saturation constants. (B) Relationship between the NO_3^- concentrations and cell count ratios of *Prochlorococcus* and *Synechococcus* in HOT. (C) The effect of doubled NO_3^- recourse. The plot shows the model results of the *Prochlorococcus* and *Synechococcus* ratio in terms of cellular N (N_{Pro}/N_{Syn}, see the color bar for values). Here, the resource ratio of $NO_3^-:NH_4^+$ is 2:3. Dashed curves indicate borders within which the coexistence occurs when the resource ratio of $NO_3^-:NH_4^+$ is 1:3 (same dashed curves as in Fig. 4A). The cyan triangle represents the ratios of predicted half-saturation constants for Fig. 2. (D) NO_3^- concentration shifts predicted by various climate models (see Materials and Methods). The y-axis represents the fractional (%) change in surface nutrient concentration throughout the low latitudes (30°S-30°N, 0-50m).

Sargasso Sea (37). The stimulation of *Synechococcus* photosynthetic and growth activity after 20 nM NO_3^- enrichment was later confirmed by an *in situ* bioassay experiment (38). While additional NH_4^+ input could have been added by the heterotrophic community or diazotrophs, the effect of extra NH_4^+ must have been small compared with 100 nM enrichment during our experiment and is unlikely to significantly affect our hypothesis (Fig. 1; Fig. S2). Taxon-specific differences in phytoplankton mortality could also be present, but their potential role in coexistence cannot be constrained by available data.

Shifts in the resource ratio $NO_3^-:NH_4^+$ can also alter the range of species traits that permit coexistence (Fig. 5C). When the NO_3^- resource increases, the range of coexistence (iv in Fig. 4B; hereafter called domain iv) shifts to the left, favoring lower $K_{NO3}^{Pro}/K_{NO3}^{Syn}$ and $K_{NH4}^{Pro}/K_{NH4}^{Syn}$ for coexistence (Fig. 5C). On the other hand, when the NH_4^+ resource increases, the domain iv shifts to the right, favoring higher $K_{NO3}^{Pro}/K_{NO3}^{Syn}$ and $K_{NH4}^{Pro}/K_{NH4}^{Syn}$ for coexistence (Fig. S6A). Due to these shifts, at an increased NO_3^- resource, we predict an increased ratio of *Synechococcus* at the predicted K values (represented by cyan triangles in Fig. 4A and Fig. 5C), and a further increase in resource ratios of $NO_3^-:NH_4^+$ eventually leads to a predominance of *Synechococcus* (Fig. 4B, 5A; Fig. S6B).

The niche partitioning of Pro/Syn based on differential preferences for reduced and oxidized forms of N has important ecological and climatic implications. The NO_3^-/NH_4^+ ratio of nutrient supply can be influenced strongly by climate change, through its impact on ocean stratification, which reduces the supply of NO_3^- to the photic zone of the low latitudes (40). This trend is supported by various climate modeling showing decreased NO_3^- concentration in low latitude euphotic zones (Fig. 5D). According to our ecological modeling, such climate changes are likely to shift the community composition of these major biomes toward a greater preponderance of *Prochlorococcus* than that of *Synechococcus* (Fig. 5A). While long-term trends are not available to test this prediction, it is consistent with perturbations observed on shorter time scales in response to transient increases of surface NO_3^- (2, 41).

However, how strongly climate change may alter the supply ratio of NO_3^- to NH_4^+ contains substantial uncertainties, partially due to the difficulty in simulating NH_4^+ in the ocean (42). The preference of NO_3^- by *Synechococcus* cannot be explained by the snapshot of vertical distribution in oligotrophic waters (39) being a marked *Prochlorococcus* abundance peak just above the nitracline, while for *Synechococcus*, the abundance peak is low all along the vertical profile (43, 44). This finding suggests we consider the nutrient history of phytoplankton, namely, frequency, scale, and duration of nutrient input (45). In fact, monthly observations at the Bermuda Atlantic Time-series Study (BATS) (2), as well as in the Gulf of Aqaba, Red Sea (41), observed spring blooms of *Synechococcus* when the water column was deeply mixed and the NO_3^- supply from deep was active and observed *Prochlorococcus* domination during summer stratification, consistent with our model predictions (Fig. 5A). Increased primary production supported by *Synechococcus* in upwelling cyclonic eddies was reported from BATS (46) and off California (47), further supporting model simulations (Fig. 5A).

The predicted and observed preference of NO_3^- by *Synechococcus* is qualitatively consistent with phylogenomic analysis, where *Synechococcus* possesses genes encoding both nitrate reductase (*narB*) and nitrite reductase (*nirA*), whereas these genes are patchy among *Prochlorococcus* strains (Fig. 6) (10, 19, 48–50). In addition to inorganic N, both *Prochlorococcus* and *Synechococcus* are capable of the uptake of organic forms of nitrogen, such as urea, similar to or better than NH_4^+ or NO_3^- (19, 51), as well as amino acids (52–56) using high-affinity amino acid transporters at low ambient N concentrations (57–59). Culture studies of *Synechococcus* showed light-stimulated incorporation of amino acids (60). In addition, the presence of genes encoding transporters of organic compounds varies among strains of marine picocyanobacteria (55). In general, the amino acid incorporation was similar to or greater in *Prochlorococcus* than that of *Synechococcus* (55, 56). Further studies to estimate the effect of organic nitrogen on their growth will be important.

Changes in the NO_3^-/NH_4^+ supply ratio can be altered by ecological changes in addition to climatic changes. The low N environments dominated by these taxa are also prime habitats for N_2-fixing diazotrophs, which inject newly fixed NH_4^+ into surface waters. The presence of N_2-fixing organisms that provide NH_4^+ may favor *Prochlorococcus*, due to its lower K value for NH_4^+, and as a result, *Synechococcus* may be outcompeted. This dynamic may underlie the correlations between *Prochlorococcus* and the filamentous diazotroph *Trichodesmium* reported from the oligotrophic South Pacific Ocean (61). Similarly, a positive relationship between *Prochlorococcus* and the unicellular diazotroph *Crocosphaera* has been suggested by showing analogous nutrient limitation in both *Crocosphaera* and *Prochlorococcus* (62), promoting the coexistence of these organisms. Distributions of both *Prochlorococcus* and *Crocosphaera* also show a positive correlation with temperature in oligotrophic oceans (3, 63). On the other hand, a negative relationship between the abundance of *Synechococcus* and nano-sized cyanobacteria (most likely *Crocosphaera*) (64) has been reported in the Pacific Ocean. Rising surface temperatures, rising atmospheric CO_2 concentrations, and strengthened water-column stratification (65) may favor diazotrophs (63, 66–68) in the future, supporting the predictions of *Prochlorococcus* domination (3) (Fig. 5A).

Overall, our observation-model synthesis suggests that the coexistence of the major marine phytoplankton is sustained by the differentiated nitrogen uptake. We were able to obtain this implication based on the high-precision measurement of nutrient concentration at nanomolar levels. Given the nutrient-depleted nature of the oligotrophic ocean and the shift in the nitrogen preference of *Synechococcus* from NO_3^- to NH_4^+ at the nanomolar level, we propose that the high-precision measurements and studies focused on the nanomolar level concentrations are essential for elucidating the ecological dynamics and biogeochemical process in the oligotrophic ocean and predicting their future shift.

Different uptake affinity to N in the content of picocyanobacterial evolution. Marine *Synechococcus* and *Prochlorococcus* are estimated to have sequentially diverged
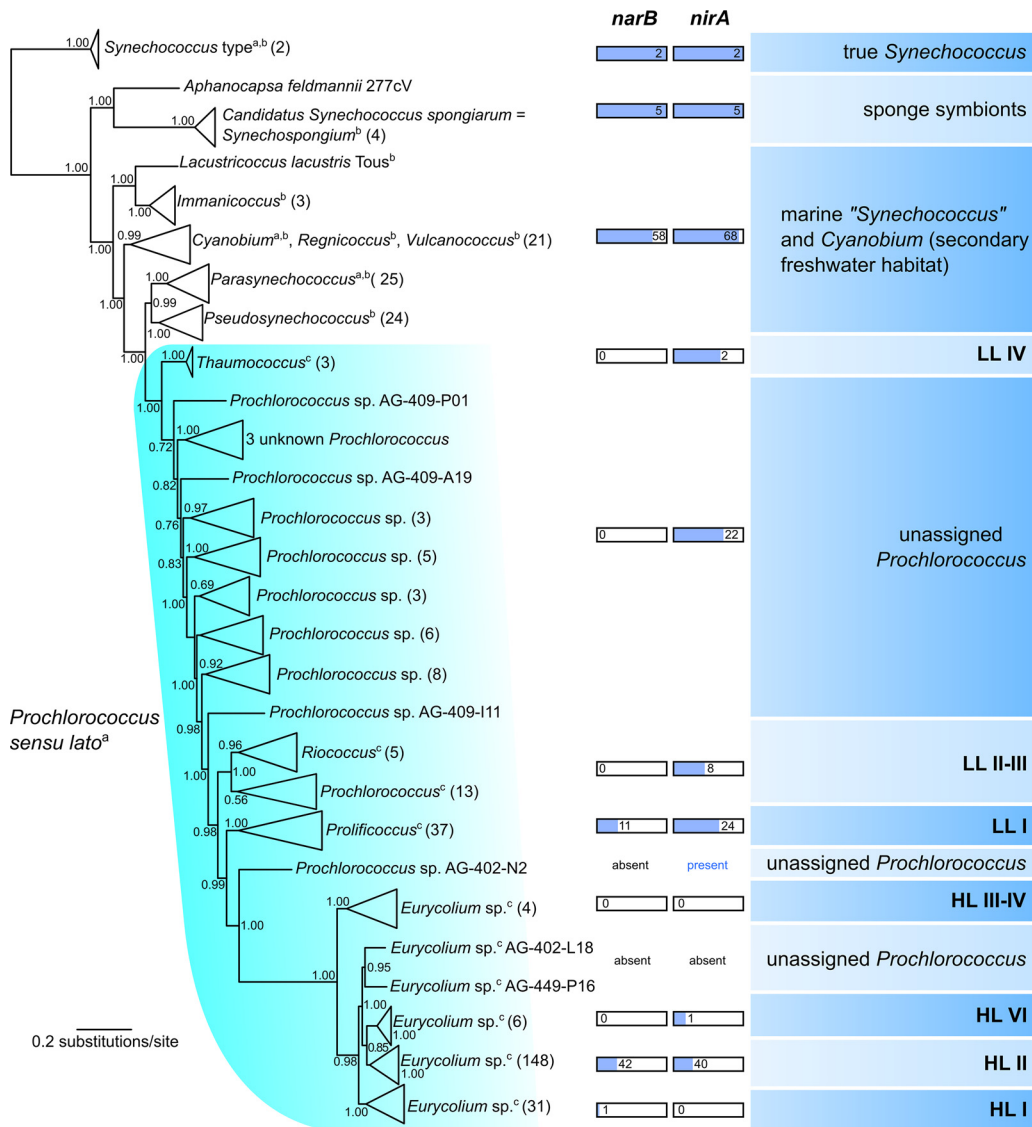
FIG 6 Phylogenomic tree of marine picocyanobacteria. The tree is rooted by the freshwater core cluster of *Synechococcus* (type strain *S. elongatus* PCC 6301). Individual clades are annotated following the most recent taxonomic revisions. The a, b, and c in superscript in the figure represent references 70–72, respectively. Phylogenetic lineages are further classified using ecological groups of *Synechococcus* and *Prochlorococcus* (right); LL and HL stand for low-light- and high-light-adapted subclades of *Prochlorococcus* (18). The multigenus clade traditionally considered *Prochlorococcus sensu lato* is highlighted in cyan. The presence of genes encoding nitrate reductase (*narB*) and nitrite reductase (*nirA*) was assessed for the individual ecological groups and expressed using the total number of occurrences within the group along with a relative abundance scale bar. The tree is based on 120 conserved bacterial proteins using the approximately maximum likelihood method following the GTDB-Tk *de novo* pipeline (92). Bootstrap values are shown near the nodes, and numbers in brackets indicate the number of genomes within collapsed clades.

from a common ancestor during the Devonian, at about 413 million years ago (Mya), and Carboniferous, at around 360 Mya and 341 Mya, respectively (69). During these periods, a number of genus-level lineages likely evolved within both *Synechococcus* (e.g., *Parasynechococcus*, "*Pseudosynechococcus*") and *Prochlorococcus* (e.g., "*Thaumococcus*," "*Prolificoccus*," "*Riococcus*," and "*Eurycolium*") (70–72). Our reconstruction suggests that many other putative genera are still waiting to be recognized (Fig. 6). These lineages are in many aspects cryptic due to morphological simplification and genome streamlining, which are driven by convergent selective pressures, especially the nutrient deficiency addressed in this study (49). Nevertheless, individual ecotypes and even individual cells of picocyanobacteria harbor distinct sets of metabolic genes reflecting their ecological niche partitioning (73–75).

The ability to assimilate NO_3^- is observed to vary widely among picocyanobacteria. Whereas most genomes of marine *Synechococcus* harbor both nitrate reductase and nitrite reductase genes, these genes exhibit a patchy distribution throughout both low-light and high-light adapted *Prochlorococcus* lineages (18, 50) (Fig. 6). According to previous studies, gene loss, as well as homologous recombination among closely related cell populations, is frequent in the genomic regions responsible for NO_3^- acquisition in *Prochlorococcus* (50). Nitrate assimilation is energetically demanding and thus more likely to occur under high-light conditions near the water surface, but the concentration of NO_3^- tends to increase with depth in oligotrophic oceans. This trade-off likely shapes the composition of *Prochlorococcus* populations by creating an equilibrium of NO_3^- assimilating and nonassimilating subpopulations that coexist at a given depth and light intensity to maximize the effectivity of N uptake (50).

Phylogenomic analysis (Fig. 6) implies that mixed populations of NO_3^- assimilating or nonassimilating "*Prochlorococcus*" cells corresponding to several different genus-level lineages may further influence the relative affinity of *Prochlorococcus* to different N substrates. This finding could be another mechanism underlying the coexistence of *Prochlorococcus* and *Synechococcus*, and their various phylogenetic sublineages, at different concentrations of available N forms. The relative contribution of genomic population diversity versus physiological affinity to specific forms of N to the coexistence of both picocyanobacteria was not addressed in the current study and thus warrants further investigation. With regard to the differential phylogeographic distribution of individual picocyanobacterial genotypes and ecotypes (76, 77), care must be taken when extrapolating the findings to oceanic regions outside Northwest Pacific, in which the verification of our hypothesis is still required.

Conclusions. Our study provides a quantitative explanation for the well-known coexistence of *Prochlorococcus* and *Synechococcus* and a new experimentally based test of a central prediction in the long-standing theory of resource competition. Nanomolar-scale nutrient addition captures the subtle but clear difference in nitrogen usage by these two organisms. We have used the data to parameterize a simple ecological model, showing that the specialization of nitrogen use (NO_3^- versus NH_4^+) leads to the coexistence of these organisms. The model also predicts shifts in the balance of competing species across a range of resource supply ratios, yielding the exclusion of *Prochlorococcus* or *Synechococcus* at high and low ratios of NO_3^-: NH_4^+, respectively. These model predictions resemble measured variations in species abundances and their covariation with NO_3^- and are also qualitatively consistent with previous observations of physical phenomena that naturally perturb the supply ratio of reduced to oxidized N. Evaluating the predicted shifts in the niche of these dominant phytoplankton will require the incorporation of differential nutrient specialization and nutrient resource fluxes in global biogeochemistry and climate models.

MATERIALS AND METHODS

Observations and experiments. A series of bioassay experiments was carried out using natural phytoplankton assemblages collected at a station in the subtropical Northwestern Pacific (12°N, 135°E) from 6 to 25 June 2008 during the MR08-02 cruise on the R/V *MIRAI*. Detailed experimental procedures are described in reference 16. Five macronutrient (N and P)-addition bioassays (M1 to M5) and three Fe-addition bioassays (Fe1 to Fe3) were conducted to elucidate the availability and preference of natural phytoplankton communities for N, P, and Fe sources (Table S7 and S8 in reference 16).

Seawater collection. Water samples were collected from a 10-m depth at 12:30 h local time using Teflon diaphragm pump system consisting of Teflon tubing and associated plastic ware. All components of this pump system and associated plastic were washed overnight in a neutral detergent, washed with HCl and HNO_3, rinsed with heated Milli-Q water, and flushed with seawater for 30 min immediately prior to sample collection. For the nutrient-addition bioassays, 4-L polycarbonate incubation bottles and other plastic instruments were rinsed overnight in a neutral detergent, followed by 0.3 N HCl, and rinsed with Milli-Q water. For Fe-addition experiments, the 2-L polycarbonate incubation bottles had been cleaned according to reference 78. Other polyethylene and Teflon lab wares were cleaned according to reference 79. All washing procedures were carried out in an onshore class-1000 clean air room, and plastic gloves were worn during these operations.

To reduce grazing pressure, we prefiltrated seawater samples prior to the bioassay setup. For the bioassay treatments with N and P addition, water was filtered through an acid-cleaned 1-μm in-line

cartridge filter (Micropore EU, ORGANO). For Fe additions, seawater was prefiltered through a 10-μm filter of the same manufacturer. The prefiltered water was then dispensed into the corresponding bioassay incubation bottles.

Iron concentrations of the seawater were measured as total iron (TFe), on the whole water samples collected directly from the pump system, and as dissolved iron (DFe), on the 125 mL of seawater collected in low-density polyethylene bottles (Nalgen; Nalge Nunc International) and filtered through an acid-cleaned 0.22-μm pore filter (Millipack-100; Millipore). All TFe and DFe samples were acidified with HCl to pH <1.5 and stored at room temperature for at least 1 year.

Triplicate samples for the NO_3^- + NO_2^- (N+N), NH_4^+, urea and soluble reactive phosphorus (SRP) (12, 80) analysis were collected in 100 mL of 0.1 N HCl-rinsed polyethylene bottles. All samples were analyzed onboard, with the exception of urea, which was measured only in the urea treatment. Upon collection, all samples were stored at −20°C until analysis.

Nutrient addition bioassay set up and incubation. A total of eight bioassays were carried out, of which five were macronutrient bioassays with additions of different forms of nitrogen or phosphate (M1 to M5) and three were Fe-addition bioassays (Fe1 to Fe3). For macronutrient bioassays, prefiltered seawater was dispensed into 4-L polycarbonate bottles. Five different triplicate treatments were set up, as follows: one control without nutrient addition; three treatments with 100 nM addition of N, whether as $NaNO_3$, NH_4Cl, or urea; and one treatment with 10 nM NaH_2PO_4 (P). Bottles were incubated on deck in flow-through seawater tanks covered with a neutral density screen to attenuate light intensity to 50% of its corresponding surface value. Macronutrient bioassays lasted 3 days with daily sample collections to follow changes in phytoplankton pigments by high-pressure liquid chromatography (HPLC) and community composition by flow cytometry (FCM). For the Fe-addition bioassays, the filtrate was poured into 2-L polycarbonate bottles that had been cleaned according to methods of reference 78. Five duplicate treatments were set up, as follows: controls without any nutrient addition, phosphate additions with 10 nM NaH_2PO_4, iron addition with 1 nM $FeCl_3$, an Fe+P treatment with 1 nM $FeCl_3$ and 10 nM NaH_2PO_4, and Fe+N treatment with amendment of 1 nM $FeCl_3$ and 100 nM $NaNO_3$. To all treatments containing iron addition, EDTA (1 nM) was added as a buffer. Fe-addition treatments were done in an onboard class-100 clean air room. Bottles for the iron-addition bioassays were also incubated in on-deck flow-through seawater tanks covered with a neutral density screen to attenuate light intensity to 50% of its corresponding surface value. Iron-addition bioassays lasted for 5 days, monitoring TFe, DFe, and phytoplankton community composition on days 0, 1, 3, and 5.

Macronutrient analysis. Concentrations of NO_3^- + NO_2^- (N+N), NH_4^+, SRP, and urea were measured using a high-sensitivity colorimetric approach with an autoanalyzer II instrument (Technicon) and liquid waveguide capillary cells (World Precision Instruments, USA) as outlined (13). Urea concentrations were analyzed by the diacetyl monoxime method (81). Detection limits of NO_3^- + NO_2^-, NH_4^+, and SRP were 3, 6, and 3 nM, respectively.

TFe and DFe concentrations. Dissolved Fe(III) in seawater samples was determined using catalytic cathodic stripping voltammetry with a detection limit of 6 pM using the approach of reference 82. No contamination during sampling and incubation was detected.

Flow cytometry (FCM). *Prochlorococcus* and *Synechococcus* were identified using flow cytometry (FCM) based on cell size and chlorophyll or phycoerythrin fluorescence. Aliquots of 4.5 mL were preserved in glutaraldehyde (1% final concentration), flash frozen in liquid N_2, and stored at −80°C until analysis by flow cytometer (PAS-III; Partec, GmbH, Münster, Germany) equipped with a 488-nm argon-ion excitation laser (100 mW) on land. Forward- and side-angle scatter (FSC and SSC, respectively), red fluorescence (>630 nm, FL3), and orange fluorescence (570 to 610 nm, FL2) were recorded. *Synechococcus* and *Prochlorococcus* were distinguished using FloMax (Partec, GmbH) based on their autofluorescence properties and their size.

Statistical analysis. Phytoplankton cell densities of each bioassay were first compared between treatments using repeated measures analysis of variance (RM-ANOVA) with nutrient treatments as the between-subjects factor (5 levels) and time (4 levels) as the within-subjects factor. Treatment effects were considered significant if the P value was <0.05. Then, means between five treatments were compared by a *post hoc* Turkey test (n = 3 replicates per treatment throughout, degrees of freedom = 40).

The ecological model of *Prochlorococcus* and *Synechococcus*. The model follows simple balances of cell densities and nutrient concentrations as used in resource competition theory (6, 7, 21, 22). This theory is suitable for predicting the ecological niches of phytoplankton in aquatic systems, such as diatoms (7) and N_2 fixers (6, 21, 22), based on different nutrient uptake behavior. We used the following four key equations:

$$\frac{dX_{Pro}}{dt} = \left(V_{maxNO3}^{Pro} \frac{[NO_3^-]}{[NO_3^-] + K_{NO3}^{Pro}} + V_{maxNH4}^{Pro} \frac{[NH_4^+]}{[NH_4^+] + K_{NH4}^{Pro}} - m_{Pro} \right) X_{Pro} \tag{1}$$

$$\frac{dX_{Syn}}{dt} = \left(V_{maxNO3}^{Syn} \frac{[NO_3^-]}{[NO_3^-] + K_{NO3}^{Syn}} + V_{maxNH4}^{Syn} \frac{[NH_4^+]}{[NH_4^+] + K_{NH4}^{Syn}} - m_{Syn} \right) X_{Syn} \tag{2}$$

$$\frac{d[NO_3^-]}{dt} = -V_{maxNO3}^{Pro} \frac{[NO_3^-]}{[NO_3^-] + K_{NO3}^{Pro}} Q_N^{Pro} X_{Pro} - V_{maxNO3}^{Syn} \frac{[NO_3^-]}{[NO_3^-] + K_{NO3}^{Syn}} Q_N^{Syn} X_{Syn} + S_{NO3} \tag{3}$$

$$\frac{d[NH_4^+]}{dt} = -V_{maxNH4}^{Pro} \frac{[NH_4^+]}{[NH_4^+] + K_{NH4}^{Pro}} Q_N^{Pro} X_{Pro} - V_{maxNH4}^{Syn} \frac{[NH_4^+]}{[NH_4^+] + K_{NH4}^{Syn}} Q_N^{Syn} X_{Syn} + S_{NH4} \qquad (4)$$

where X_i (cell L^{-1}) = abundance of phytoplankton i (i = Pro, Syn; *Prochlorococcus* and *Synechococcus*, respectively)

t (d) = time

V_{maxj}^i (d^{-1}) = maximum uptake rate of phytoplankton i for nutrient j ($j = NO_3^-$, NH_4^+)

$[j]$ (nmol L^{-1}) = nutrient concentration

K_j^i (nmol L^{-1}) = half-saturation constant of nutrient j for phytoplankton i

m_i (d^{-1}) = mortality rate of phytoplankton i

Q_N^i (nmol cell^{-1}) = cellular nitrogen content of phytoplankton i

S_j (nmol L^{-1} d^{-1}) = resource term for nutrient j

The cell densities are the outcome of the balances between cellular growth and mortality (equation 1 and 2). The balances of NO_3^- and NH_4^+ are represented by the uptake by cells and a constant source of each nutrient (equation 3 and 4). For Q_N^i, we used the average values from experiments M1 to M3, which were estimated based on the FCM-analyzed cell size with the reference carbon per cell volume (83) and carbon-to-nitrogen ratios (84). We first manually parameterized V_{maxj}^i, K_j^i, m_i, and S_j as well as initial values for X_i and $[j]$ (hereafter, predicted parameters) in order for X_i and $[j]$ to closely represent observations (Fig. 2; Fig. S3). After that step, we applied the Metropolis-Hastings algorithm (85, 86) as used in reference 87 and 88 to improve the parameterization of V_{maxj}^i, K_j^i, and m_i. Parameter values and initial values are in Table S4 and S6, respectively. We limited the application of the algorithm to these parameters because the number of parameters is already large. After the parameters were selected, we solved these equations under the steady state to obtain X_i values using Mathematica 11.3 (89) and plotted $Q_N^{Pro} X_{Pro} / Q_N^{Syn} X_{Syn}$ for different resource ratios (Fig. 4A, 5A, 5C; Fig. S6). Because the equations are based on the existence of these two organisms, valid solutions are obtained only where these organisms coexist. For Fig. 4A and 5C and Fig. S6A and B, we varied the ratios of half-saturation constants, using NO_3^-: NH_4^+ resource ratios of 1:3, 2:3, 1:6, and 3:1, respectively.

We chose these equation formulas given the currently available data. The addition of NH_4^+ and NO_3^- may not strictly represent the physiology these organisms. For example, there are finer-scale intracellular molecular interactions than those represented here. For example, NO_3^- may become a source for NH_4^+, and maximum growth rate may be constrained separately. Despite the simplification, however the model reproduced the population data (Fig. 2) under N limitation, which accounts for a large part of the *Prochlorococcus* and *Synechococcus* habitats (3, 90). Thus, we hypothesized that more detailed intracellular mechanisms may have only a secondary effect. Resolving intracellular mechanisms would require a number of additional parameters, which may not be as well constrained as those we use here; further experiments would be required for more detailed physiological analyses.

Nutrient trend analysis. We analyzed surface nutrient trends from projections of future climate states under the Representative Concentration Pathway (RCP) 8.5 greenhouse gas emissions scenarios from 5 different Earth System Models (ESMs) participating in the Climate Model Intercomparison Project (CMIP5) (91) (see Table S7 in the supplemental material). The past and future climate trajectories in ESMs are forced by historical greenhouse gas emissions until the early 21st century and then by the RCP8.5 emissions scenario, which reaches a nominal radiative forcing of 8.5 W/m^2 in 2100 (Table S7).

Phylogenetic analysis. To assess the evolutionary history of picocyanobacteria, we constructed a phylogenetic tree utilizing a *de novo* workflow available in the Genome Taxonomy Database (GTDB) toolkit (92, 93). GTDB-Tk v1.3.0, employing the R05-RS95 release of GTDB from July 2020, was used to produce a standardized approximately maximum likelihood phylogenomic tree (FastTree2) (94) based on 120 concatenated conserved bacterial markers. The tree spanned all known genome-sequenced picocyanobacterial clades and was rooted by a closely related outgroup taxon, *Synechococcus elongatus*. To assess the potential of picocyanobacteria to assimilate NO_3^- (and nitrite: NO_2^-), all genomes included in the analysis were screened for the presence of the nitrate reductase (*narB*) and ferredoxin-nitrite reductase (*nirA*) genes. The search for *narB* and *nirA* homologues was performed using BLASTp and tBLASTn with query proteins mined from *S. elongatus* PCC 6301 (genome accession AP008231.1) and default parameters; the resulting hits were verified using the conserved domain search available in NCBI (95). Taxonomic grouping of picocyanobacteria was annotated following recent studies (70–72), and individual phylogenetic lineages were subsequently assigned to the traditional ecological scheme of low-light- versus high-light-adapted ecotypes (10, 50). Table S8 shows a list of strains and genome assemblies used for phylogenomic reconstruction in Fig. 6, and their placement in clades as dipicted therein.

Code availability. The model has been written in Python 3 and is freely available in Zenodo online at https://zenodo.org/record/4568561.

Data availability. The data used to generate the graphs presented in the main figures can be found in Data Set S1 in the supplemental material or online at Zenodo (https://zenodo.org/record/4568561). All other data that support the findings of this study are available on request from the corresponding author.

SUPPLEMENTAL MATERIAL

Supplemental material is available online only.

SUPPLEMENTAL FILE 1, XLSX file, 0.01 MB.

SUPPLEMENTAL FILE 2, PDF file, 1.9 MB.

ACKNOWLEDGMENTS

REFERENCES

1. Field C, Behrenfeld MJ, Randerson JT, Falkowski P. 1998. Primary production of the biosphere: integrating terrestrial and oceanic components. Science 281:237–240. https://doi.org/10.1126/science.281.5374.237.
2. DuRand MD, Olson RJ, Chisholm SW. 2001. Phytoplankton population dynamics at the Bermuda Atlantic Time-series station in the Sargasso Sea. Deep Sea Res II 48:1983–2003. https://doi.org/10.1016/S0967-0645(00)00166-1.
3. Flombaum P, Gallegos JL, Gordillo RA, Rincon J, Zabala LL, Jiao N, Karl DM, Li WKW, Lomas MW, Veneziano D, Vera CS, Vrugt JA, Martiny AC. 2013. Present and future global distributions of the marine Cyanobacteria *Prochlorococcus* and *Synechococcus*. Proc Natl Acad Sci U S A 110: 9824–9829. https://doi.org/10.1073/pnas.1307701110.
4. Partensky F, Hess WR, Vaulot D. 1999. *Prochlorococcus*, a marine photosynthetic prokaryote of global significance. Microbiol Mol Biol Rev 63: 106–127. https://doi.org/10.1128/MMBR.63.1.106-127.1999.
5. Hutchinson GE. 1961. The paradox of the plankton. The Am Nat 95:137–145. https://doi.org/10.1086/282171.
6. Ward BA, Dutkiewicz S, Moore CM, Follows MJ. 2013. Iron, phosphorus, and nitrogen supply ratios define the biogeography of nitrogen fixation. Limnol Oceanogr 58:2059–2075. https://doi.org/10.4319/lo.2013.58.6.2059.
7. Tilman D. 1977. Resource competition between plankton algae: an experimental and theoretical approach. Ecology 58:338–348. https://doi.org/10.2307/1935608.
8. Hashihama F, Yasuda I, Kumabe A, Sato M, Sasaoka H, Iida Y, Shiozaki T, Saito H, Kanda J, Furuya K, Boyd PW, Ishii M. 2021. Nanomolar phosphate supply and its recycling drive net community production in the subtropical North Pacific. Nat Commun 12:3462. https://doi.org/10.1038/s41467-021-23837-y.
9. Tilman D. 1982. Resource competition and community structure. Princeton University Press, Princeton, NJ.
10. Martiny AC, Kathuria S, Berube PM. 2009. Widespread metabolic potential for nitrite and nitrate assimilation among *Prochlorococcus* ecotypes. Proc Natl Acad Sci U S A 106:10787–10792. https://doi.org/10.1073/pnas.0902532106.
11. Dutkiewicz S, Hickman AE, Jahn O, Gregg WW, Mouw CB, Follows MJ. 2015. Capturing optically important constituents and properties in a marine biogeochemical and ecosystem model. Biogeosciences 12:4447–4481. https://doi.org/10.5194/bg-12-4447-2015.
12. Karl DM, Björkman KM, Dore JE, Fujieki L, Hebel DV, Houlihan T, Letelier RM, Tupas LM. 2001. Ecological nitrogen-to-phosphorus stoichiometry at station ALOHA. Deep Sea Res II 48:1529–1566. https://doi.org/10.1016/S0967-0645(00)00152-1.
13. Hashihama F, Furuya K, Kitajima S, Takeda S, Takemura T, Kanda J. 2009. Macro-scale exhaustion of surface phosphate by dinitrogen fixation in the western North Pacific. Geophys Res Lett 36:L03610. https://doi.org/10.1029/2008GL036866.
14. Kodama T, Furuya K, Hashihama F, Takeda S, Kanda J. 2011. Occurrence of rain-origin nitrate patches at the nutrient-depleted surface in the East China Sea and the Philippine Sea during summer. J Geophys Res 116:C08003. https://doi.org/10.1029/2010JC006814.
15. Ackermann M. 2015. A functional perspective on phenotypic heterogeneity in microorganisms. Nat Rev Microbiol 13:497–508. https://doi.org/10.1038/nrmicro3491.
16. Masuda T, Inomura K, Kodama T, Shiozaki T, Kitajima S, Armin G, Matsui T, Suzuki K, Takeda S, Sato M, Prášil O, Furuya K. 2022. *Crocosphaera* as a major consumer of fixed nitrogen. Microbiol Spectr 10:e02177-21. https://doi.org/10.1128/spectrum.02177-21.
17. Shilova IN, Mills MM, Robidart JC, Turk-Kubo KA, Björkman KM, Kolber Z, Rapp I, van Dijken GL, Church MJ, Arrigo KR, Achterberg EP, Zehr JP. 2017. Differential effects of nitrate, ammonium, and urea as N sources for microbial communities in the North Pacific Ocean. Limnol Oceanogr 62:2550–2574. https://doi.org/10.1002/lno.10590.
18. Berube PM, Biller SJ, Kent AG, Berta-Thompson JW, Roggensack SE, Roache-Johnson KH, Ackerman M, Moore LR, Meisel JD, Sher D, Thompson LR, Campbell L, Martiny AC, Chisholm SW. 2015. Physiology and evolution of nitrate acquisition in *Prochlorococcus*. ISME J 9:1195–1207. https://doi.org/10.1038/ismej.2014.211.
19. Moore LR, Post AF, Rocap G, Chisholm SW. 2002. Utilization of different nitrogen sources by the marine cyanobacteria *Prochlorococcus* and *Synechococcus*. Limnol Oceanogr 47:989–996. https://doi.org/10.4319/lo.2002.47.4.0989.
20. Glibert PM, Ray RT. 1990. Different patterns of growth and nitrogen uptake in two clones of marine *Synechococcus* spp. Mar Biol 107:273–280. https://doi.org/10.1007/BF01319826.
21. Dutkiewicz S, Ward BA, Monteiro F, Follows MJ. 2012. Interconnection of nitrogen fixers and iron in the Pacific Ocean: theory and numerical simulations. Global Biogeochem Cycles 26:GB1012. https://doi.org/10.1029/2011GB004039.
22. Dutkiewicz S, Ward BA, Scott JR, Follows MJ. 2014. Understanding predicted shifts in diazotroph biogeography using resource competition theory. Biogeosciences 11:5445–5461. https://doi.org/10.5194/bg-11-5445-2014.
23. Armstrong RA. 2008. Nutrient uptake rate as a function of cell size and surface transporter density: a Michaelis-like approximation to the model of Pasciak and Gavis. Deep Sea Res Part I: Oceanogr Res Papers 55:1311–1317. https://doi.org/10.1016/j.dsr.2008.05.004.

24. Smith SL, Yamanaka Y, Pahlow M, Oschlies A. 2009. Optimal uptake kinetics: physiological acclimation explains the pattern of nitrate uptake by phytoplankton in the ocean. Mar Ecol Prog Ser 384:1–12. https://doi.org/10.3354/meps08022.

25. Bonachela JA, Raghib M, Levin SA. 2011. Dynamic model of flexible phytoplankton nutrient uptake. Proc Natl Acad Sci U S A 108:20633–20638. https://doi.org/10.1073/pnas.1118012108.

26. Healey FP. 1980. Slope of the Monod equation as an indicator of advantage in nutrient competition. Microb Ecol 5:281–286. https://doi.org/10.1007/BF02020335.

27. Van de Waal DB, Litchman E. 2020. Multiple global change stressor effects on phytoplankton nutrient acquisition in a future ocean. Philos Trans R Soc Lond B Biol Sci 375:20190706. https://doi.org/10.1098/rstb.2019.0706.

28. Hirata T, Hardman-Mountford NJ, Brewin RJW, Aiken J, Barlow R, Suzuki K, Isada T, Howell E, Hashioka T, Noguchi-Aita M, Yamanaka Y. 2011. Synoptic relationships between surface chlorophyll-a; and diagnostic pigments specific to phytoplankton functional types. Biogeosciences 8:311–327. https://doi.org/10.5194/bg-8-311-2011.

29. Christaki U, Courties C, Karayanni H, Giannakourou A, Maravelias C, Kormas KA, Lebaron P. 2002. Dynamic characteristics of *Prochlorococcus* and *Synechococcus* consumption by bacterivorous nanoflagellates. Microb Ecol 43:341–352. https://doi.org/10.1007/s00248-002-2002-3.

30. Avrani S, Wurtzel O, Sharon I, Sorek R, Lindell D. 2011. Genomic island variability facilitates *Prochlorococcus*-virus coexistence. Nature 474:604–608. https://doi.org/10.1038/nature10172.

31. Marston MF, Pierciey FJ, Jr, Shepard A, Gearin G, Qi J, Yandava C, Schuster SC, Henn MR, Martiny JB. 2012. Rapid diversification of coevolving marine *Synechococcus* and a virus. Proc Natl Acad Sci U S A 109:4544–4549. https://doi.org/10.1073/pnas.1120310109.

32. Vallina SM, Ward BA, Dutkiewicz S, Follows MJ. 2014. Maximal feeding with active prey-switching: a kill-the-winner functional response and its effect on global diversity and biogeography. Prog Oceanogr 120:93–109. https://doi.org/10.1016/j.pocean.2013.08.001.

33. Ward BA, Dutkiewicz S, Follows MJ. 2014. Modelling spatial and temporal patterns in size-structured marine plankton communities: top–down and bottom–up controls. J Plankton Res 36:31–47. https://doi.org/10.1093/plankt/fbt097.

34. Dutkiewicz S, Cermeno P, Jahn O, Follows MJ, Hickman AE, Taniguchi DAA, Ward BA. 2020. Dimensions of marine phytoplankton diversity. Biogeosciences 17:609–634. https://doi.org/10.5194/bg-17-609-2020.

35. Follows MJ, Dutkiewicz S, Ward BA, Follett CN. 2018. Theoretical interpretation of subtropical plankton biogeography, p 467. *In* Gasol J, Kirshman D (eds), Microbial ecology of the oceans, 3rd ed. John Wiley, Hoboken, NJ.

36. Karl DM, Lukas R. 1996. The Hawaii Ocean Time-series (HOT) program: background, rationale and field implementation. Deep-Sea Res 43:129–156. https://doi.org/10.1016/0967-0645(96)00005-7.

37. Glover HE, Prézelin BB, Campbell L, Wyman M, Garside C. 1988. A nitrate-dependent *Synechococcus* bloom in surface Sargasso Sea water. Nature 331:161–163. https://doi.org/10.1038/331161a0.

38. Glover HE, Garside C, Trees CC. 2007. Physiological responses of Sargasso Sea picoplankton to nanomolar nitrate perturbations. J Plankton Res 29:263–274. https://doi.org/10.1093/plankt/fbm013.

39. Partensky F, Blanchot J, Vaulot D. 1999. Differential distribution and ecology of *Prochlorococcus* and *Synechococcus* in oceanic waters: a review. Bull Inst Oceanogr 19:457–475.

40. Bograd SJ, Jacox MG, Hazen EL, Lovecchio E, Montes I, Pozo Buil M, Shannon LJ, Sydeman WJ, Rykaczewski RR. 2023. Climate change impacts on eastern boundary upwelling systems. Annu Rev Mar Sci 15:303–328. https://doi.org/10.1146/annurev-marine-032122-021945.

41. Lindell D, Post AF. 1995. Ultraphytoplankton succession is triggered by deep winter mixing in the Gulf of Aqaba (Eilat), Red Sea. Limnol Oceanogr 40:1130–1141. https://doi.org/10.4319/lo.1995.40.6.1130.

42. Paulot F, Jacob DJ, Johnson MT, Bell TG, Baker AR, Keene WC, Lima ID, Doney SC, Stock CA. 2015. Global oceanic emission of ammonia: constraints from seawater and atmospheric observations. Global Biogeochem Cycles 29:1165–1178. https://doi.org/10.1002/2015GB005106.

43. Olson RJ, Chisholm SW, Zettler ER, Altabet MA, Dusenberry JA. 1990. Spatial and temporal distributions of prochlorophyte picoplankton in the North Atlantic Ocean. Deep Sea Res 37:1033–1051. https://doi.org/10.1016/0198-0149(90)90109-9.

44. Campbell L, Vaulot D. 1993. Photosynthetic picoplankton community structure in the subtropical North Pacific Ocean near Hawaii (station ALOHA). Deep Sea Res 40:2043–2060. https://doi.org/10.1016/0967-0637(93)90044-4.

45. Droop MR. 1973. Some thoughts on nutrient limitation in algae. J Phycol 9:264–272. https://doi.org/10.1111/j.1529-8817.1973.tb04092.x.

46. Sweeney EN, McGillicuddy DJ, Buesseler KO. 2003. Biogeochemical impacts due to mesoscale eddy activity in the Sargasso Sea as measured at the Bermuda Atlantic Time-series Study (BATS). Deep Sea Res Part II Top Stud Oceanogr 50:3017–3039. https://doi.org/10.1016/j.dsr2.2003.07.008.

47. Paerl RW, Johnson KS, Welsh RM, Worden AZ, Chavez FP, Zehr JP. 2011. Differential distributions of *Synechococcus* subgroups across the California current system. Front Microbiol 2:59. https://doi.org/10.3389/fmicb.2011.00059.

48. Scanlan DJ, Ostrowski M, Mazard S, Dufresne A, Garczarek L, Hess WR, Post AF, Hagemann M, Paulsen I, Partensky F. 2009. Ecological genomics of marine picocyanobacteria. Microbiol Mol Biol Rev 73:249–299. https://doi.org/10.1128/MMBR.00035-08.

49. Partensky F, Garczarek L. 2010. *Prochlorococcus*: advantages and limits of minimalism. Annu Rev Mar Sci 2:305–331. https://doi.org/10.1146/annurev-marine-120308-081034.

50. Berube PM, Rasmussen A, Braakman R, Stepanauskas R, Chisholm SW. 2019. Emergence of trait variability through the lens of nitrogen assimilation in *Prochlorococcus*. Elife 8:e14043. https://doi.org/10.7554/eLife.41043.

51. Casey JR, Lomas MW, Mandecki J, Walker DE. 2007. *Prochlorococcus* contributes to new production in the Sargasso Sea deep chlorophyll maximum. Geophys Res Let 34:L10604. https://doi.org/10.1029/2006GL028725.

52. Zubkov MV, Fuchs BM, Tarran GA, Burkill PH, Amann R. 2003. High rate of uptake of organic nitrogen compounds by *Prochlorococcus* cyanobacteria as a key to their dominance in oligotrophic oceanic waters. Appl Environ Microbiol 69:1299–1304. https://doi.org/10.1128/AEM.69.2.1299-1304.2003.

53. Zubkov MV, Tarran GA, Fuchs BM. 2004. Depth related amino acid uptake by *Prochlorococcus* cyanobacteria in the Southern Atlantic tropical gyre. FEMS Microbiol Ecol 50:153–161. https://doi.org/10.1016/j.femsec.2004.06.009.

54. Garcia-Fernandez JM, de Marsac NT, Diez J. 2004. Streamlined regulation and gene loss as adaptive mechanisms in *Prochlorococcus* for optimized nitrogen utilization in oligotrophic environments. Microbiol Mol Biol Rev 68:630–638. https://doi.org/10.1128/MMBR.68.4.630-638.2004.

55. Muñoz-Marín MC, Gómez-Baena G, López-Lozano A, Moreno-Cabezuelo JA, Díez J, García-Fernández JM. 2020. Mixotrophy in marine picocyanobacteria: use of organic compounds by *Prochlorococcus* and *Synechococcus*. ISME J 14:1065–1073. https://doi.org/10.1038/s41396-020-0603-9.

56. Michelou VK, Cottrell MT, Kirchman DL. 2007. Light-stimulated bacterial production and amino acid assimilation by cyanobacteria and other microbes in the North Atlantic Ocean. Appl Environ Microbiol 73:5539–5546. https://doi.org/10.1128/AEM.00212-07.

57. Stoecker DK, Hansen PJ, Caron DA, Mitra A. 2017. Mixotrophy in the marine plankton. Annu Rev Mar Sci 9:311–335. https://doi.org/10.1146/annurev-marine-010816-060617.

58. Rocap G, Larimer FW, Lamerdin J, Malfatti S, Chain P, Ahlgren NA, Arellano A, Coleman M, Hauser L, Hess WR, Johnson ZI, Land M, Lindell D, Post AF, Regala W, Shah M, Shaw SL, Steglich C, Sullivan MB, Ting CS, Tolonen A, Webb EA, Zinser ER, Chisholm SW. 2003. Genome divergence in two *Prochlorococcus* ecotypes reflects oceanic niche differentiation. Nature 424:1042–1047. https://doi.org/10.1038/nature01947.

59. Zubkov MV, Tarran GA. 2005. Amino acid uptake of *Prochlorococcus* spp. in surface waters across the South Atlantic Subtropical Front. Aquat Microb Ecol 40:241–249. https://doi.org/10.3354/ame040241.

60. Pearl H. 1991. Ecophysiological and trophic implications of light-stimulated amino acid utilization in marine picoplankton. Appl Environ Microbiol 57:473–479. https://doi.org/10.1128/aem.57.2.473-479.1991.

61. Shiozaki T, Bombar D, Riemann L, Sato M, Hashihama F, Kodama T, Tanita I, Takeda S, Saito H, Hamasaki K, Furuya K. 2018. Linkage between dinitrogen fixation and primary production in the oligotrophic South Pacific Ocean. Glob Biogeochem Cycles 32:1028–1044. https://doi.org/10.1029/2017GB005869.

62. Moisander PH, Zhang R, Boyle EA, Hewson I, Montoya JP, Zehr JP. 2012. Analogous nutrient limitations in unicellular diazotrophs and *Prochlorococcus* in the South Pacific Ocean. ISME J 6:733–744. https://doi.org/10.1038/ismej.2011.152.

63. Moisander PH, Beinart RA, Hewson I, White AE, Johnson KS, Carlson CA, Montoya JP, Zehr JP. 2010. Unicellular cyanobacterial distributions broaden the oceanic N$_2$ fixation domain. Science 327:1512–1514. https://doi.org/10.1126/science.1185468.

64. Sato M, Hashihama F, Kitajima S, Takeda S, Furuya K. 2010. Distribution of nano-sized Cyanobacteria in the western and central Pacific Ocean. Aquat Microb Ecol 59:273–282. https://doi.org/10.3354/ame01397.

65. IPCC. 2007. Climate change 2007: the physical science basis. Cambridge University Press, New York, NY.

66. Fu F-X, Mulholland MR, Garcia NS, Beck A, Bernhardt PW, Warner ME, Sañudo-Wilhelmy SA, Hutchins DA. 2008. Interactions between changing pCO_2, N_2 fixation, and Fe limitation in the marine unicellular cyanobacterium *Crocosphaera*. Limnol Oceanogr 53:2472–2484. https://doi.org/10.4319/lo.2008.53.6.2472.

67. Hutchins DA, Fu F-X, Zhang Y, Warner ME, Feng Y, Portune K, Bernhardt PW, Mulholland MR. 2007. CO_2 control of *Trichodesmium* N_2 fixation, photosynthesis, growth rates, and elemental ratios: implications for past, present, and future ocean biogeochemistry. Limnol Oceanogr 52:1293–1304. https://doi.org/10.4319/lo.2007.52.4.1293.

68. Fu FX, Yu E, Garcia NS, Gale J, Luo Y, Webb EA, Hutchins DA. 2014. Differing responses of marine N_2 fixers to warming and consequences for future diazotroph community structure. Aquat Microb Ecol 72:33–46. https://doi.org/10.3354/ame01683.

69. Sánchez-Baracaldo P, Bianchini G, Di Cesare A, Callieri C, Chrismas NAM. 2019. Insights into the evolution of picocyanobacteria and phycoerythrin genes (mpeBA and cpeBA). Front Microbiol 10:45. https://doi.org/10.3389/fmicb.2019.00045.

70. Komárek J, Johansen JR, Šmarda J, Strunecký O. 2020. Phylogeny and taxonomy of *Synechococcus*-like cyanobacteria. Fottea 20:171–191. https://doi.org/10.5507/fot.2020.006.

71. Tschoeke D, Salazar VW, Vidal L, Campeão M, Swings J, Thompson F, Thompson C. 2020. Unlocking the genomic taxonomy of the *Prochlorococcus* collective. Microb Ecol 80:546–558. https://doi.org/10.1007/s00248-020-01526-5.

72. Salazar VW, Tschoeke DA, Swings J, Cosenza CA, Mattoso M, Thompson CC, Thompson FL. 2020. A new genomic taxonomy system for the *Synechococcus* collective. Environ Microbiol 22:4557–4570. https://doi.org/10.1111/1462-2920.15173.

73. Kashtan N, Roggensack SE, Rodrigue S, Thompson JW, Biller SJ, Coe A, Ding H, Marttinen P, Malmstrom RR, Stocker R, Follows MJ, Stepanauskas R, Chisholm SW. 2014. Single-cell genomics reveals hundreds of coexisting subpopulations in wild *Prochlorococcus*. Science 344:416–420. https://doi.org/10.1126/science.1248575.

74. Biller SJ, Berube PM, Lindell D, Chisholm SW. 2015. *Prochlorococcus*: the structure and function of collective diversity. Nat Rev Microbiol 13:13–27. https://doi.org/10.1038/nrmicro3378.

75. Doré H, Farrant GK, Guyet U, Haguait J, Humily F, Ratin M, Pitt FD, Ostrowski M, Six C, Brillet-Guéguen L, Hoebeke M, Bisch A, Le Corguillé G, Corre E, Labadie K, Aury JM, Wincker P, Choi DH, Noh JH, Eveillard D, Scanlan DJ, Partensky F, Garczarek L. 2020. Evolutionary mechanisms of long-term genome diversification associated with niche partitioning in marine picocyanobacteria. Front Microbiol 11:567431. https://doi.org/10.3389/fmicb.2020.567431.

76. Zwirglmaier K, Jardillier L, Ostrowski M, Mazard S, Garczarek L, Vaulot D, Not F, Massana R, Ulloa O, Scanlan DJ. 2008. Global phylogeography of marine *Synechococcus* and *Prochlorococcus* reveals a distinct partitioning of lineages among oceanic biomes. Environ Microbiol 10:147–161. https://doi.org/10.1111/j.1462-2920.2007.01440.x.

77. Doré H, Leconte J, Guyet U, Breton S, Farrant GK, Demory D, Ratin M, Hoebeke M, Corre E, Pitt FD, Ostrowski M, Scanlan DJ, Partensky F, Six C, Garczarek L. 2022. Global phylogeography of marine *Synechococcus* in coastal areas reveals strong community shifts. mSystems 7:e00656-22. https://doi.org/10.1128/msystems.00656-22.

78. Takeda S, Obata H. 1995. Response of equatorial Pacific phytoplankton to subnanomolar Fe enrichment. Mar Chem 50:219–227. https://doi.org/10.1016/0304-4203(95)00037-R.

79. Obata H, Karatani H, Nakayama E. 1993. Automated determination of iron in seawater by chelating resin concentration and chemiluminescence detection. Anal Chem 65:1524–1528. https://doi.org/10.1021/ac00059a007.

80. Wu J, Sunda W, Boyle EA, Karl DM. 2000. Phosphate depletion in the western North Atlantic Ocean. Science 289:759–762. https://doi.org/10.1126/science.289.5480.759.

81. Price NM, Harrison PJ. 1987. Comparison of methods for the analysis of dissolved urea in seawater. Mar Biol 94:307–317. https://doi.org/10.1007/BF00392945.

82. Laglera LM, Santos-Echeandia J, Caprara S, Monticelli D. 2013. Quantification of iron in seawater at the low picomolar range based on optimization of bromate/ammonia/dihydroxynaphtalene system by catalytic adsorptive cathodic stripping voltammetry. Anal Chem 85:2486–2492. https://doi.org/10.1021/ac303621q.

83. Shalapyonok A, Olson RJ, Shalapyonok LS. 2001. Arabian Sea phytoplankton during Southwest and Northeast Monsoon 1995: composition, size structure and biomass from individual cell properties measured by flow cytometry. Deep Sea Res II 48:1231–1261. https://doi.org/10.1016/S0967-0645(00)00137-5.

84. Heldal M, Scanlan DJ, Norland S, Thingstad F, Mann NH. 2003. Elemental composition of single cells of various strains of marine *Prochlorococcus* and *Synechococcus* using X-ray microanalysis. Limnol Oceanogr 48:1732–1743. https://doi.org/10.4319/lo.2003.48.5.1732.

85. Hastings WK. 1970. Monte Carlo sampling methods using Markov chains and their applications. Biometrika 57:97–109. https://doi.org/10.1093/biomet/57.1.97.

86. Metropolis N, Rosenbluth AW, Rosenbluth MN, Teller AH. 1953. Equation of state calculations by fast computing machines. J Chem Phys 2:1087–1092.

87. Inomura K, Omta AW, Talmy D, Bragg J, Deutsch C, Follows MJ. 2020. A Mechanistic model of macromolecular allocation, elemental stoichiometry, and growth rate in phytoplankton. Front Microbiol 11:86. https://doi.org/10.3389/fmicb.2020.00086.

88. Omta AW, Talmy D, Sher D, Finkel ZV, Irwin AJ, Follows MJ. 2017. Extracting phytoplankton physiological traits from batch and chemostat culture data. Limnol Oceanogr Methods 15:453–466. https://doi.org/10.1002/lom3.10172.

89. Wolfram Research Inc. 2018. Mathematica, version 11.3. Wolfram Research Inc., Champaign, IL.

90. Moore CM, Mills MM, Arrigo KR, Berman-Frank I, Bopp L, Boyd PW, Galbraith ED, Geider RJ, Guieu C, Jaccard SL, Jickells TD, La Roche J, Lenton TM, Mahowald NM, Marañón E, Marinov I, Moore JK, Nakatsuka T, Oschlies A, Saito MA, Thingstad TF, Tsuda A, Ulloa O. 2013. Processes and patterns of oceanic nutrient limitation. Nature Geosci 6:701–710. https://doi.org/10.1038/ngeo1765.

91. Taylor KE, Stouffer RJ, Meehl GA. 2012. An overview of CMIP5 and the experiment design. Bull Am Meteorol Soc 93:485–498. https://doi.org/10.1175/BAMS-D-11-00094.1.

92. Chaumeil PA, Mussig AJ, Hugenholtz P, Parks DH. 2020. GTDB-Tk: a toolkit to classify genomes with the Genome Taxonomy Database. Bioinformatics 36:1925–1927. https://doi.org/10.1093/bioinformatics/btz848.

93. Parks DH, Chuvochina M, Chaumeil PA, Rinke C, Mussig AJ, Hugenholtz P. 2020. A complete domain-to-species taxonomy for Bacteria and Archaea. Nat Biotechnol 38:1079–1086. https://doi.org/10.1038/s41587-020-0501-8.

94. Price MN, Dehal PS, Arkin AP. 2010. FastTree 2—approximately maximum-likelihood trees for large alignments. PLoS One 5:e9490. https://doi.org/10.1371/journal.pone.0009490.

95. Marchler-Bauer A, Bryant SH. 2004. CD-Search: protein domain annotations on the fly. Nucleic Acids Res 32:W327–W331. https://doi.org/10.1093/nar/gkh454.

96. Kudo I, Harrison PJ. 1997. Effect of iron nutrition on the marine cyanobacterium *Synechococcus* grown on different N sources and irradiances. J Phycol 33:232–240. https://doi.org/10.1111/j.0022-3646.1997.00232.x.